International Journal of Civil Engineering

Structure - Concrete

Numerical simulation of concrete fracture under compression by explicit discrete element method

R. Abbasnia[1,*], M. Aslami

Received: June 2014, Revised: September 2014, Accepted: December 2014

Abstract

A new model is proposed for two-dimensional simulation of the concrete fracture in compression. The model generated by using the Voronoi diagram method and with considering random shape and distribution of full graded aggregates at the mesoscopic level. The aggregates modeled by combining irregular polygons, which then is placed into the concrete with no intersection between them. By this new modeling approach, the simulation of high-strength concretes with possible aggregates fracture is also feasible. After generation of the geometrical model, a coupled explicit discrete element method and a modified rigid body spring model have been used for solution. In this method, all the neighboring elements are connected by springs. The mortar springs have Elasto-plastic behavior and considering normal concrete, the aggregate springs behave only elastically without any fracture. The proposed model can accurately predict the mechanical behavior of concrete under compression for small and large deformations both descriptively and quantitatively.

Keywords: *Concrete fracture, Numerical simulation, Explicit discrete element method, Voronoi diagram, Mesoscale simulation.*

1. Introduction

Concrete is perhaps the most common manufactured materials. The low cost, wide availability, ease of use and high durability of concrete has led to its continually increasing usage in construction technology. It can be a hastily prepared, low-grade mixture for simple applications, or a firmly controlled engineering material for high-performance structures. Complex physical and chemical interactions within the cement paste play an important role in the properties of concrete. This structure led to complicated processes in fracture formation and development. Therefore, most of the evaluations of the mechanical properties of concrete and its behavior have been performed through experimental studies [1-5]. These researches are expensive and time consuming, thus developing efficient numerical models for the simulation of concrete fracture are necessary.

The current techniques for modeling of fracture and damage within concrete and other quasi-brittle materials, can be classified into a continuum [6-9] and discrete [10-17] methods.

Continuum models provide an average description of material behavior for a representative volume element.

Because the width of the fracture process zone (FPZ) in concrete can be sizable (roughly several times the maximum aggregate size), the simulation of concrete fracture in mesoscopic levels with continuum approaches is unsuitable. Discrete micromechanical model provides fundamental knowledge about material behavior. On the other hand, if material structure (e.g. at micro/meso scale of observation) is explicitly represented, then the models can provide a direct direction for studying crack patterns, mechanisms of softening in post-peak branch, and size effect/scaling phenomena [18].

In the recent years, several approaches to model the mesostructure and the fracture process of concrete have been proposed. Rossi et al developed the probabilistic model using the finite element method to simulate the compressive behavior of concrete [19]. The main weakness of their proposed method is the determination of the compressive strength as input data for numerical analysis. Camborde et al used discrete element method (DEM) for simulation of concrete behavior [20]. Their model was relatively reliable, but only two phases for concrete (i.e. aggregate and cement) has been considered and the effects of the interface is neglected, also assumed the same stiffness for all links between the elements. In a study conducted by Nagai et al. [21], a rigid body-spring model (RBSM) is developed to simulate the failure of mortar and concrete under uniaxial and biaxial stress conditions. The results of their model were satisfactory, but the model can be used only for solving small deformation problems. Wang et al presented a two-

** Corresponding author: abbasnia@iust.ac.ir*
1 Department of Civil Engineering, Iran University of Science and Technology, Tehran 16844, Iran
2 Research assistant

[DOI: 10.22068/IJCE.13.3.245]

dimensional mesoscopic numerical method to simulate the failure process of concrete under compression based on the discrete element method and modified the rigid body-spring model [22]. This method can be used to predict the mechanical behavior of concrete under compression descriptively and quantitatively both for either small or larger deformation problems. However, to simplify the model, the aggregate was considered as one regular polygon with the same size.

The present study proposes an efficient two-dimensional geometrical model for concrete, taking into account the random shapes and distribution of full graded aggregates at the mesoscopic level. The aggregates modeled by combining irregular polygons, which is then placed into the concrete with no intersection between them. By this new modeling approach, the restrictions related to the aggregate size, shape and distribution have been removed and the simulation of high-strength concretes with possible aggregates fracture also feasible.

2. Generation of Geometry Model

The first step in the numerical simulation of materials behavior is creating a geometrical model. In the proposed model, concrete cracks initiate and propagates along the element boundary, thus the mesh arrangement can affect the fracture direction and Regular meshes, which is often used in traditional FEM, may cause cracks formation in a certain direction. Therefore, for decreasing the influence of mesh arrangements in the fracture mode of concrete, the Voronoi diagram [23] has been used to discretize the material into an assemblage of polygon elements. Let $\mathbf{V}$ be a part of two-dimensional space and $\mathbf{P} = \sum \mathbf{P_i}$ is randomly distributed points in $\mathbf{V}$ (Fig .1a). Then the Voronoi cell for point $\mathbf{P_i}$ can be constructed by partition of $\mathbf{V}$ in a way that each region of $\mathbf{V_{P_i}}$ is a set of points, which is a closer site to $\mathbf{P_i}$ than to any other sites in the plane (Fig .1b) [23].

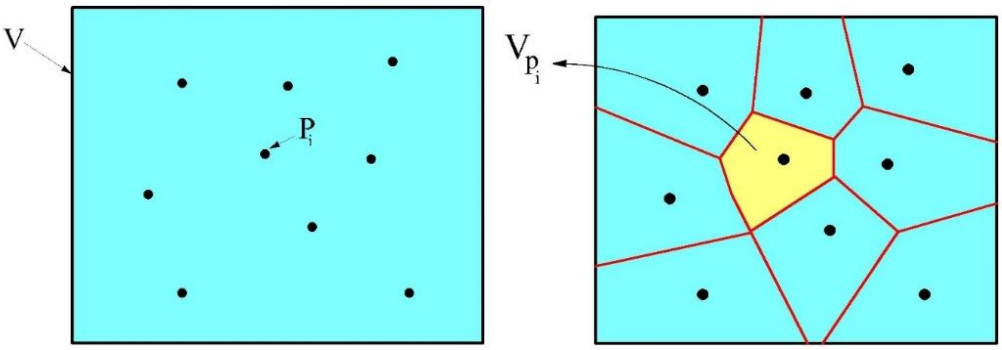

(a) Two-dimensional space ($\mathbf{V}$) and distributed points (b) Voronoi diagram and Voronoi cell for $\mathbf{P_i}$

Fig. 1 Schematic representation of Voronoi diagram

In the model, concrete is composed of aggregates and mortar elements and zero-size interfaces. For comparison with references, size-distribution diagram for aggregates has been selected from JSCE (Japan society of civil engineers) standard specification for concrete structures (Fig. 2). Average Aggregates diameters are in the range of 6 to $20\mathbf{mm}$ (millimeter), with $2\mathbf{mm}$ increments (Table. 1). The number of aggregates for each size is obtained by using the distribution curve, represented in Fig. 2. The volume of all aggregates is approximately 38% of total volume, similar to a normal concrete, and are distributed randomly in the sample [24].

Table 1 Aggregate size and percentage

Aggregate diameter (mm)	6	8	10	12	14	16	18	20
Percentage of each diameter	12 %	14 %	13 %	11 %	13 %	11 %	11 %	15 %

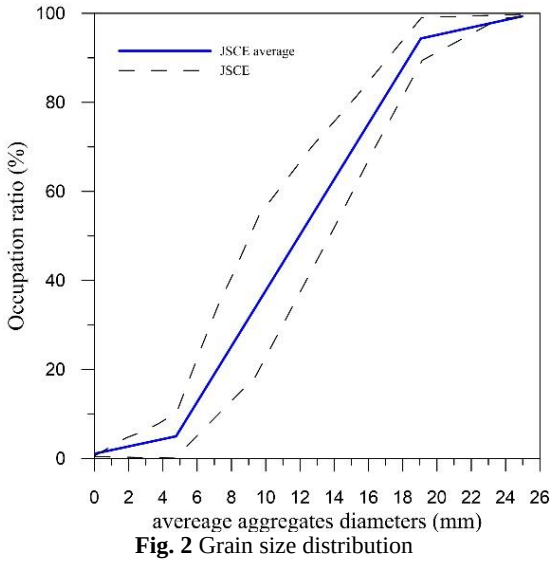

Fig. 2 Grain size distribution

2.1. Automatic mesh generation [24]

In this section an efficient two-dimensional geometrical model for concrete, which taking into account the random shapes and distribution of full graded aggregates, is presented. The new approach in this model is the consideration of the irregularity of aggregates

[DOI: 10.22068/IJCE.13.3.245]

shapes, which can be led to more realistic simulation of concrete. The following algorithm descriptively shows the systematic mesh generation of the model.

1 - Insert sample size, number of elements and the Aggregates diameter matrix (**ADM**)

Where $\mathbf{ADM} = [6,8,10,12,14,16,18,20]$ in this simulation

2- Determination of the approximate distance between centers of adjacent elements.

3- Distribution of Elements centers within the specimen and construction of incomplete specimen with Voronoi diagram (Fig. 3)

4- Adding very dense regular points around the sample for the completion of boundary elements (Fig.4)

5- Creation of the final model with straight boundary and loading plates (Fig.5)

6- Random distribution of aggregates

6-1- Elimination of the boundary elements (the boundary elements can be mortar elements only)

6-2- Random rearrangement of remaining elements

6-3- Random distribution of aggregate elements using the following algorithm:

For $\mathbf{i} = 1,\mathbf{n}$ (where **n** is the length of **ADM**, in this model **n**=8)

{

For $\mathbf{j} = 1,\mathbf{m}$ (where **m** is the number of aggregates obtained for each diameter by using of distribution diagram)

{

As **i**th aggregate center considering of **j**th element

For $\mathbf{k} = 1,\mathbf{l}$ (where **l** is the number of elements obtained in 6-1)

{

Determine the distance between the center of element **j** with respect to rest of elements

If (if the distance obtained above is less than the radius of **i**th array of ADM)

Considering all the elements entered into this section as the other elements of aggregate **i**

End

}

End

}

Remove element **j** and elements obtained for the **i**th aggregate, from the matrix created in step 6-2

End

}

End

Fig. 6 also describes the total process of geometry construction in flowchart. The complete geometry for several concrete samples with same elements and dimensions and different distributions of aggregates are shown in Fig. 7.

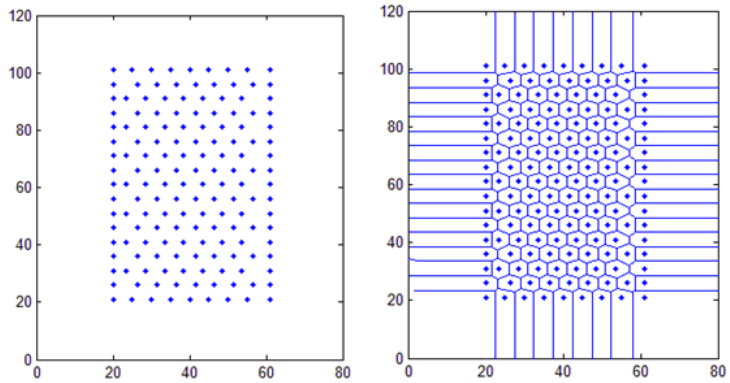

(a) Distribution of Elements center within the specimen (b) generation of the incomplete mesh

Fig. 3 First step in mesh generation

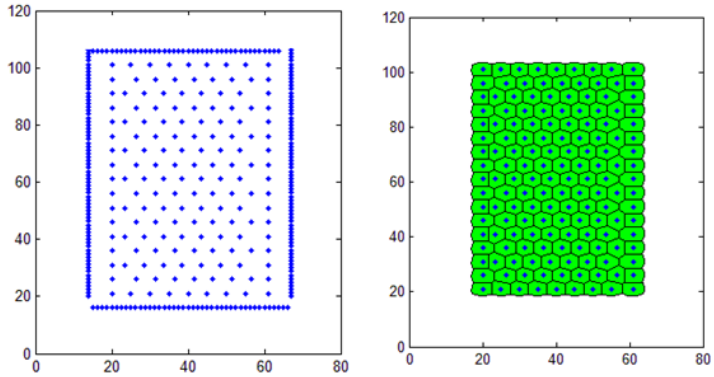

(a) Addition of very dense regular points around the sample (b) generation of the complete sample

Fig. 4 Completion of boundary elements with additional points

[DOI: 10.22068/IJCE.13.3.245]

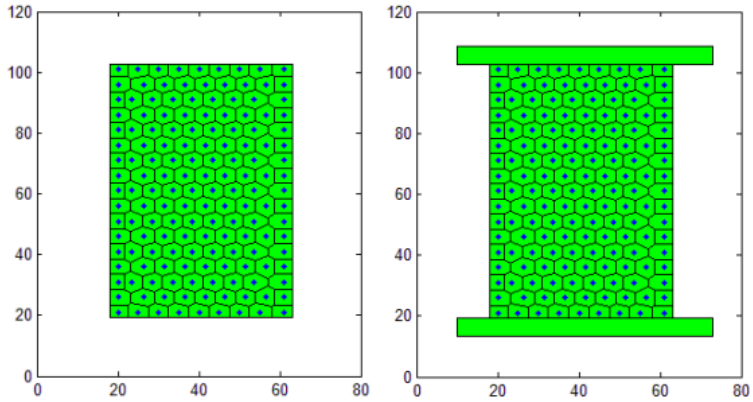

Fig. 5 Creation of the final sample

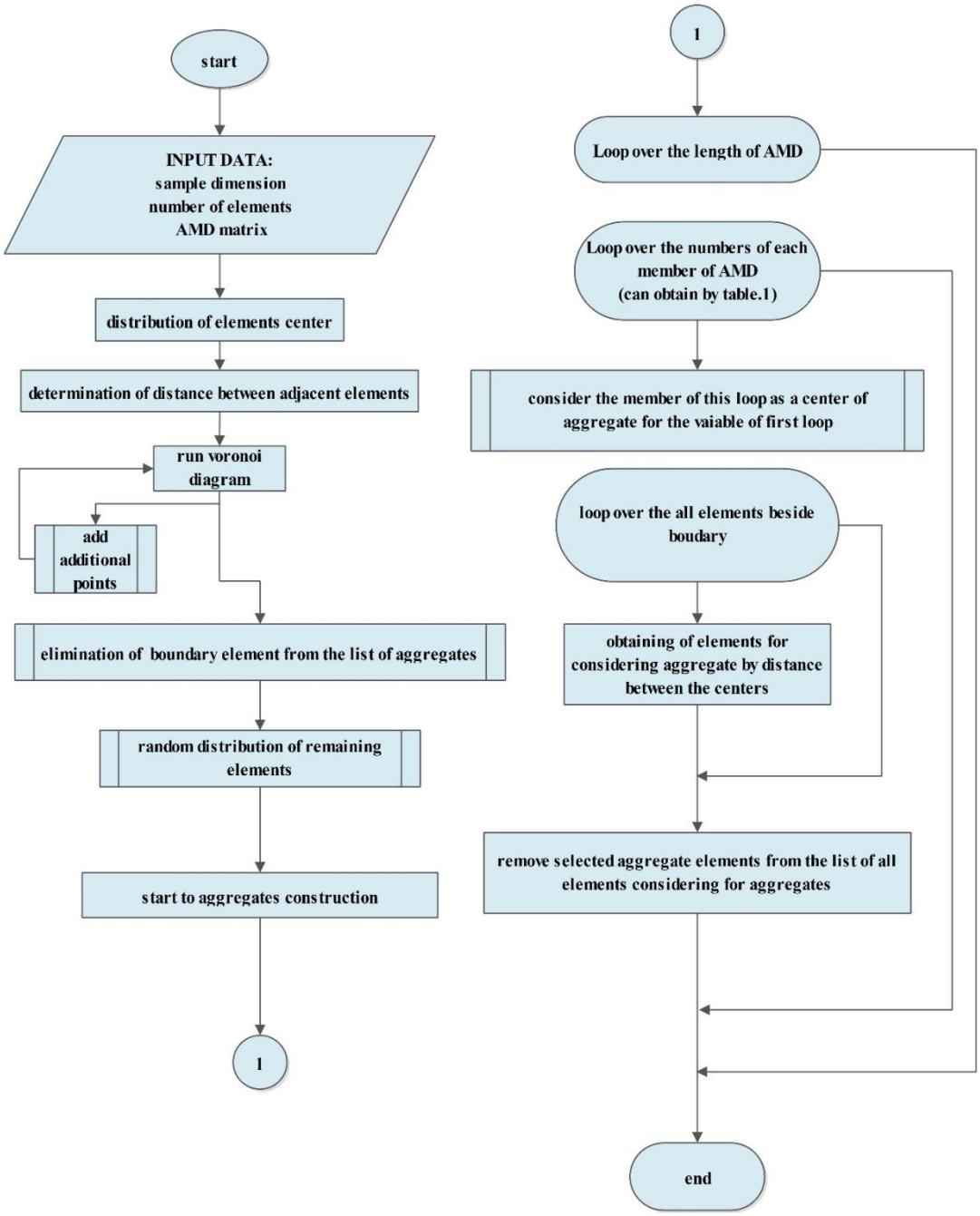

Fig. 6 total process of geometry construction

[DOI: 10.22068/IJCE.13.3.245]

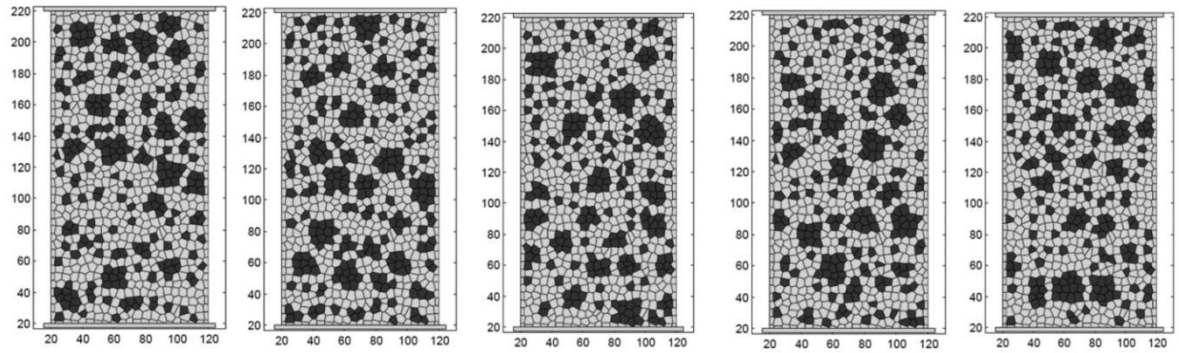

Fig. 7 The same sample with different aggregates' distributions

3. Constitutive Mechanical Model

After generation of the geometric model, the simulation process is completed by addition of mechanical relations between the elements. For this propose, the modified RBSM (rigid body-spring model) model used to, create the mechanical model. In this model, each element has one rotational and two translational degrees of freedom and all the neighboring elements are connected by normal and tangential springs. Tensile or compressive forces are transmitted by normal springs in normal direction and shear forces by shear springs in tangential direction. Three kinds of springs are defined to take the different mechanical properties of interface, mortar and aggregate into account. There are interfacial springs connecting aggregate element to mortar elements, mortar springs connecting two mortar elements, and represents deformations of mortar elements, and aggregate springs connecting two aggregate elements (Fig. 8).

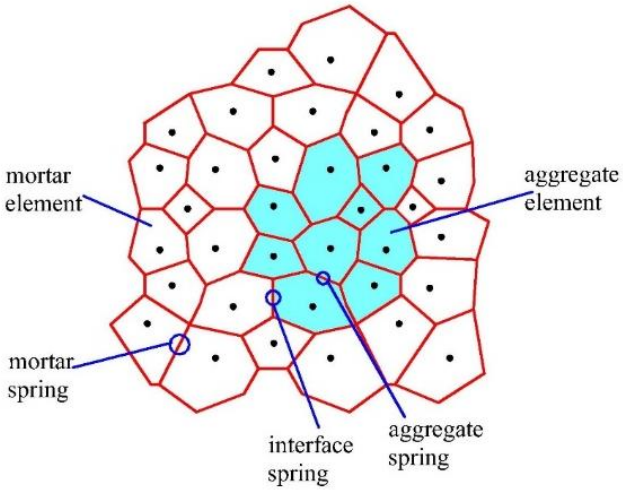

Fig. 8 Elements and springs definition

Fig. 9 describes the relation between two adjacent elements and degrees of freedom of each element as $\mathbf{u},\mathbf{v},\boldsymbol{\theta}$ (where $\mathbf{u},\mathbf{v}$ are horizontal and vertical displacements and $\boldsymbol{\theta}$ is the rotation of the element). In this figure, $\mathbf{k}_n$ &$\mathbf{k}_s$ are stiffness and $\boldsymbol{\delta}_n$ &$\boldsymbol{\delta}_s$ are deformations of normal and shear springs, respectively; $\mathbf{b}$ is the length of the common boundary of the two elements and $\mathbf{h}_1$ &$\mathbf{h}_2$ is the length of the perpendicular line from the center of gravity of adjacent elements to the common boundary [22].

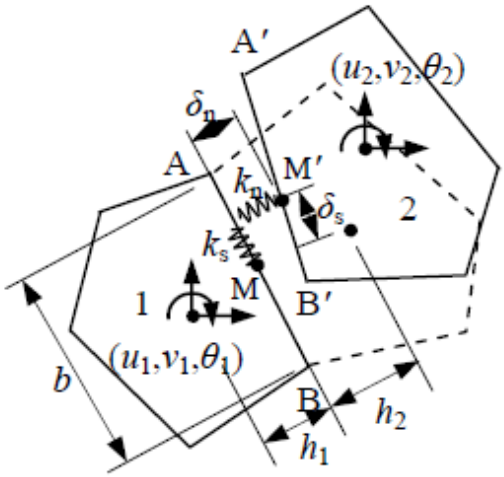

Fig. 9 Relationship of two elements [19]

3.1. Spring's behavior

Constitutive models of normal and shearing springs in a macro-scale cannot be applied to a meso-scale analysis. Therefore the model proposed by Wang et al [22], is used for constitutive model of mortar spring (Fig. 10). In Fig. 10, $w_{\max}$ is the maximum crack width, $\boldsymbol{\delta}_{c\max}$ and $\boldsymbol{\delta}_{t\max}$ are the deformation of normal spring corresponding to the maximum compressive force $F_{c\max}$ and tensile force $F_{t\max}$, and $\boldsymbol{\delta}_{s\max}$ is the deformation of shear spring corresponding to the maximum shear force $F_{s\max}$. In the simulation model, the Mohr-Coulomb criterion has been used for the failure and the $F_{s\max}$ may change with the variation of the normal force. $w_{\max}$ is set as $0.003mm$ based on the experimental results of mortar [25] and $\boldsymbol{\delta}_{c\max}$ equals to $0.002(h_1+h_2)$, where 0.002

[DOI: 10.22068/IJCE.13.3.245]

is an approximate value derived from the strain of concrete at peak compressive stress. Slopes of spring's behavior considered in plain stress condition are as in equation 1.

$$\mathbf{k_n} = \mathbf{bE_i}/((h_1+h_2)(1-\upsilon_i^2))$$
$$\mathbf{k_{-n}} = -\mathbf{F_{tmax}}/(\mathbf{w}_{max}-\boldsymbol{\delta}_{tmax}) \quad (1)$$

$\mathbf{k_s} = \mathbf{bE_i}/((h_1+h_2)(1+\upsilon_i))$, where $\mathbf{i}$ is the number of element.

In this simulation approach, only the maximum tensile stress ($F_{t\max}$) should be set as a material strength. For calculation of $F_{t\max}$ in each boundary of distinct element, the length of common boundary ($\mathbf{b}$) is multiplied to the macroscopic tensile strength of concrete. The aggregate particles constructed by several elements and since the simulation is performed on normal concrete (fracture occurs only in mortar), aggregate springs behave only elastically without fracture. The same equations as used for mortar springs are adopted to represent the material properties of the aggregates. The mechanical properties of the interface are weaker than the mortar; thus, a referenced coefficient of 0.8 is used to simulate the interface properties.

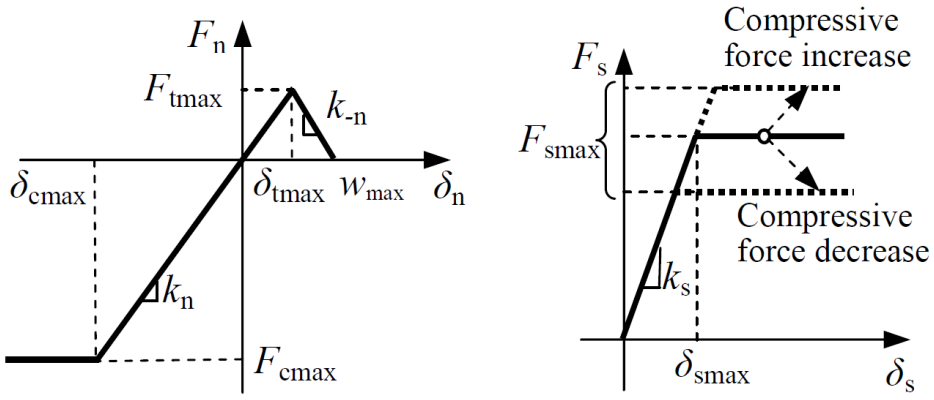

(a) Normal spring (b) Shear spring

Fig. 10 springs behavior

4. Solution of Discrete Environment

Explicit discrete element method [26] has been employed for the solution of the problem. In this method, the equilibrium contact forces and displacement of elements are determined through a series of calculations tracing the movements of the individual particles [27]. The following steps describe this technique, which can be applied to the rigid elements:

1. The rigid elements are initially unloaded and constrained to their initial positions, without causing any internal interactions.

2. When any loading applied (loads or displacements in boundary or gravity), the effect is not considered simultaneously for all elements but initially considered separately for one element after another.

3. Running the solution for one element, which is relaxed. The relaxed element is an element affected by the loads, and therefore, it will have translational and rotational movements according to the governing equations (equations of motion in this case) while all other elements remain with their initial positions and conditions. on the other hand, the constraints on the current element are removed.

4. Calculation of reaction forces between the relaxed element and its neighboring elements according to the contact laws and positions. In this step, the effect of the loading transfer from the relaxed element to the system.

5. Relaxation of neighboring elements of the current "relaxed" element (i.e., moving these elements according to the interaction forces/moments, which they received through their contacts with the currently "relaxed" element and leave initial position). The relaxation process performed for each element distinctly, therefore no set of simultaneous equations formed.

6. Repeat steps 1–5 for all elements affects by boundary loads (or all elements by gravity).

7. The resultant out-of-balance forces and moments of all elements are calculated and the relaxation continues for those elements, whose resultant out-of-balance forces and moments are larger than a preset criterion. Convergence is reached when the total out-of-balance forces and moments of the whole system is minimized.

5. Model Verification

In this section, several concrete samples under uniaxial compressive load have been simulated to verify the efficiency of the proposed model. The samples C1 and C2 considered for the comparison by the References. Therefore, the input parameters for C1 and C2 are the same as Refs. [21, 22]. C3, C4 and C5 are normal concrete samples were tested by the authors and compared by reference [28] for the investigation of aspect ratio. In the end, five specimens with the same size (H/D=2)[1] and different aggregates distributions has been considered for investigation of the effect of aggregates distributions in the

[DOI: 10.22068/IJCE.13.3.245]

behavior of specimens. The target compressive strengths are 30 MPa. The input parameters of the samples is shown in Table 2, where, $\mathbf{f_t}$, $\mathbf{E}$ and υ are the tensile strength, elastic modulus, and Poisson ratio of mortar at macro-level, respectively. The velocity of displacement on the top of the sample considered within the values of lower than 0.002 mm/s to simulate the static load condition. The time step is 2×10 −3 and 2×10 −5 s for the pre peak and post peak of the sample, respectively.

Table 2 Parameters of the samples

Specimen index	Size (height-width) (mm)	$\mathbf{f_t}$ (MPa)	**E** (MPa)	ν
C1	100×200			
C2	50×100			
C3	25×50	3.48	21876	0.18
C4	25×75			
C5	25×200			

5.1. Analysis of uniaxial compression test

The compressive strength of C1and C2, obtained from the proposed model is 28.89 MPa and 28.37 MPa, respectively. The crack mode and stress-strain curve of C1 and C2 are shown in Fig. 10.

The stress-strain curves obtained for the samples are almost similar with the RBSM (rigid body-spring model) and DEM (discrete element method) methods, but the results show more nonlinearity. The strain of the C1 and C2 at peak compressive stress is about 0.001833 and 0.002101, respectively (Figs. 11 b, d), which is more reasonable for the common concrete than 0.00 133 and 0.00175 calculated with the RBSM [21] and DEM methods [22]. The results of the present article, are more accurate in comparison with other references, due to using of full-graded aggregates with irregular shapes. Therefore, by using a more realistic model the more accurate results can be obtained.

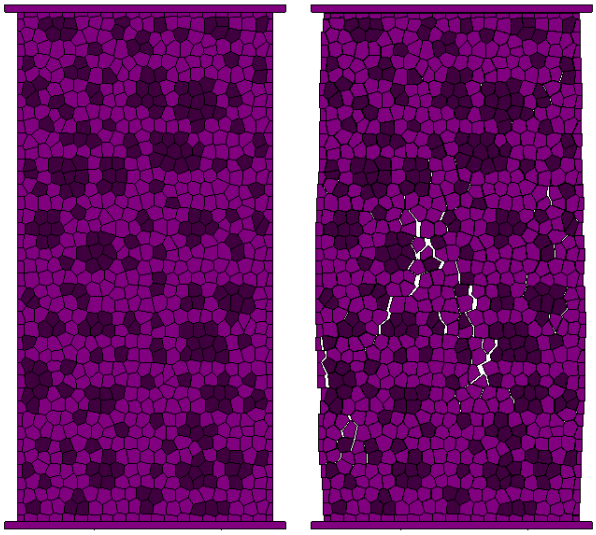

(a) Initial and crack mode of C1

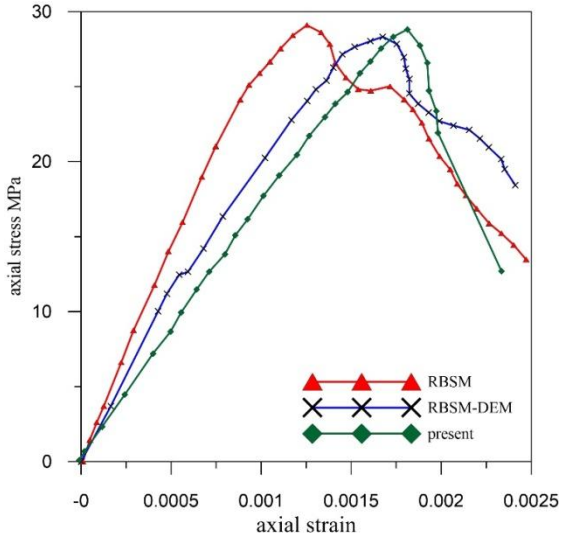

(b) Comparison between stress-strain curve of C1 and references

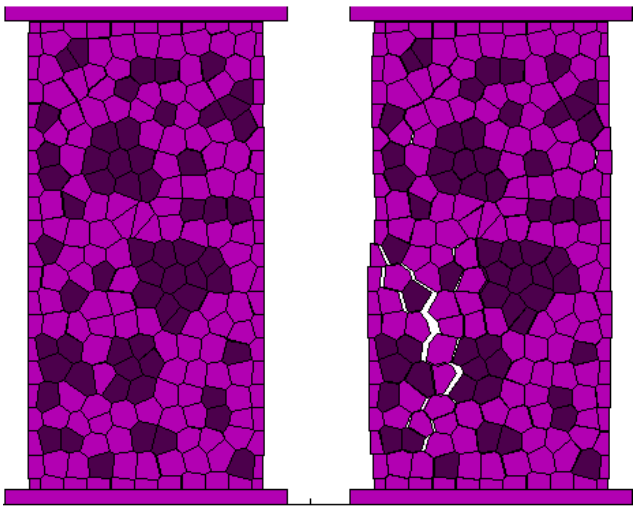

(c) Initial and crack mode of C2

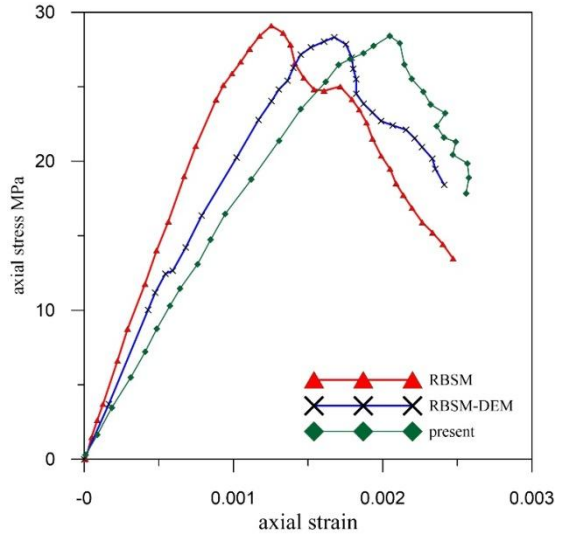

(d) Comparison between stress-strain curve of C2 and references

Fig. 11 (a-d) Results of uniaxial compression test

[DOI: 10.22068/IJCE.13.3.245]

5.2. Effect of sample dimensions

A comparative analysis is performed to determine the effect of dimensions ratio on the samples behavior. For this propose, three samples are modeled with the same input properties (Table 2). With respect to results, the general behavior of concrete specimens with different aspect ratio almost same, but the strain of the samples at the peak compressive stress decreases with increasing of H/D (Fig. 12). This phenomenon is due to tending of concrete specimens to local fracturing with increasing of H/D. Fig.13 shows crack mode of specimens with different aspect ratio and its relative experimental results [28].

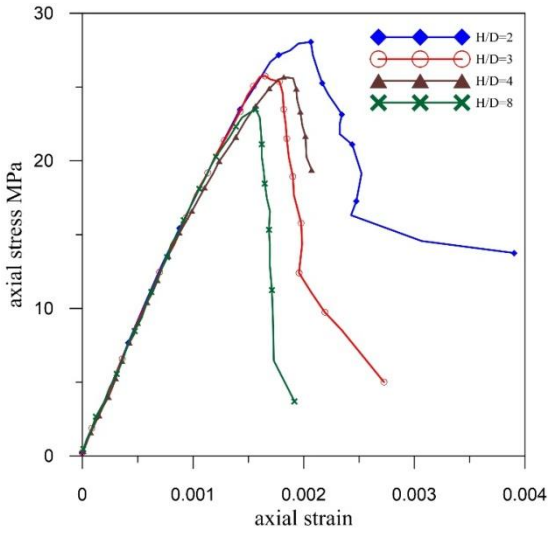

Fig. 12 Effect of the sample dimensions on the stress-strain curve

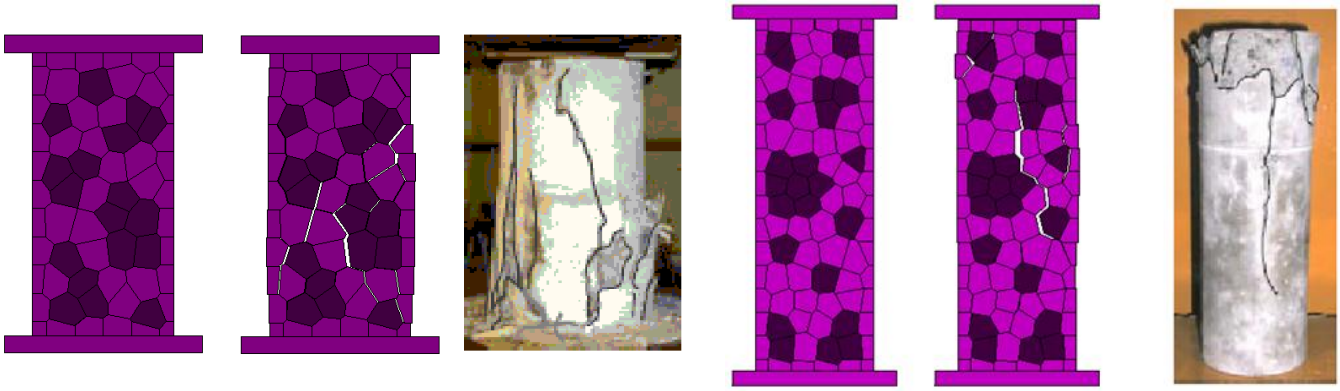

a) H/D=2 b) H/D=3

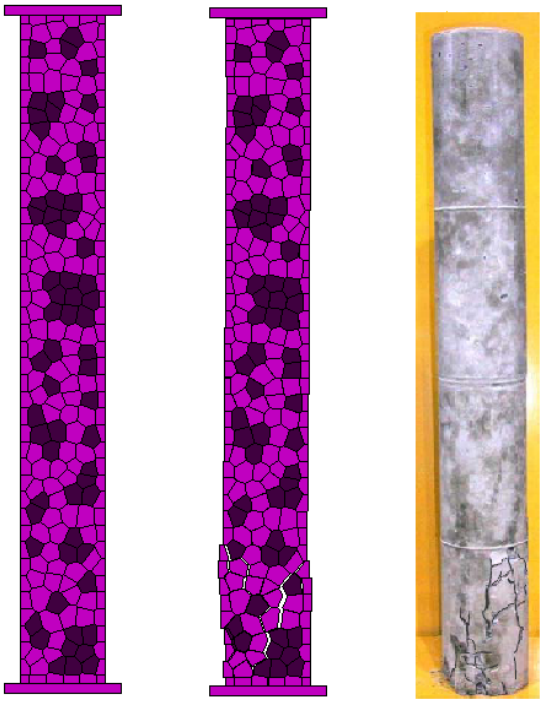

c) H/D=8

Fig. 13 Simulation of three samples with different H/D (a,b,c)

5.3. Effects of different distributions of aggregates

The effect of aggregates distributions in the behavior of

[DOI: 10.22068/IJCE.13.3.245]

specimens has been evaluated in the present section. In practical work, random distribution of aggregates is a common event. Since a fair simulation model should be reflect this fact. Therefore, for verification of the effect of aggregates distributions on stress-strain diagram of concrete, five specimens with the same size (H/D=2) and parameters has been simulated and results are summarized in Fig. 14. As it is clear from the Figure, the aggregate's distribution has a little effect on the behavior of the concrete samples.

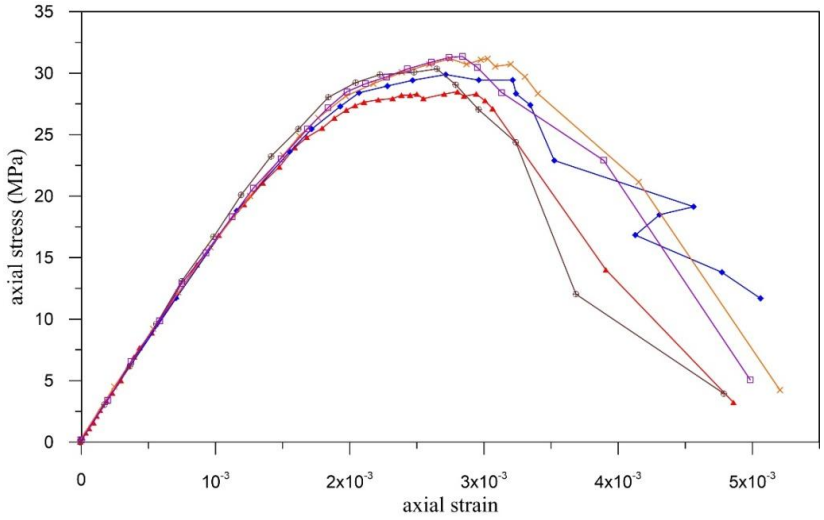

Fig. 14 Comparisons five samples with the same size and different aggregates' distributions

6. Conclusions

In this paper, a new algorithm is developed for modeling the concrete samples taking in to account the random distribution of full-graded aggregates. The aggregates are modeled by combining irregular polygons, which then are placed into the concrete with no intersection between them. By this new modeling approach, the simulation of high-strength concretes with possible aggregates fracture, is also feasible. This model predicts the strains at the peak of compressive stress which is close to the experimental results. In specimens with a different aspect ratio, the simulation also predicts cracking mode similar to experimental results. Finally, a comparison was performed among five samples with the same size and different aggregates distributions. The obtained results show that there is no significant sensitivity towards the mesh dependencies (aggregates distribution) at the maximum compressive strength and the fracture behavior of the concrete. With respect to model proposed by Wang et al [22], the results of the present article are more accurate due to using of full-graded aggregates with irregular shapes. Therefore, by using the more realistic model the more accurate results can be obtained. However, further researches should be conducted for modeling of high-strength reinforced concrete and developing an optimal programming algorithm for simulation of structural concrete members.

Note

1. height- diameter(width in two dimensional)

References

[1] Gabet T, Vu XH, Malecot Y, Daudeville L. A new experimental technique for the analysis of concrete under high triaxial loading, Journal de Physique IV, 2006, Vol. 134, pp. 635-40.

[2] Gabet T, Malcot Y, Daudeville L. Triaxial behaviour of concrete under high stresses: influence of the loading path on compaction and limit states, Cement and Concrete Research, 2008, Vol. 38, pp. 403-12.

[3] Bastami M, Aslani F, Esmaeilnia Omran M. High-temperature mechanical properties of concrete, International Journal of Civil Engineering, 2010, No. 4, Vol. 8, pp. 337-351.

[4] Abbasnia R, Holakoo A. An investigation of stress-strain behavior of FRP-confined concrete under cyclic compressive loading, International Journal of Civil Engineering, 2012, No. 3, Vol. 10, pp. 201-209.

[5] Ramadoss P. Combined effect of silica fume and steel fiber on the splitting tensile strength of high-strength concrete, International Journal of Civil Engineering, 2014, No. 1, Vol. 12, pp. 96-103.

[6] Tregger N, Corr D, Graham-Brady L, Shah S. Modeling the effect of mesoscale randomness on concrete fracture, probabilistic Engineering Mechanics, 2006, No. 3, Vol. 21, pp. 217-225.

[7] Wriggers P, Moftah SO. Mesoscale models for concrete: Homogenisation and damage behaviour, Finite Elements in Analysis and Design, 2006, No. 7, Vol. 42, pp. 623-636.

[8] Bernard F, Kamali S, Prince W. 3D multi-scale modeling of mechanical behavior of sound and leached mortar, Cement and Concrete Research, 2008, Vol. 38, pp. 449-458.

[9] Youcai Wu, Dongdong Wang, Cheng-Tang Wu. Three dimensional fragmentation simulation of concrete structures with a nodally regularized meshfree method, Theoretical and Applied Fracture Mechanics, 2014.

[10] Iturrioz, Lacidogna, Carpinteri, Experimental analysis and truss-like discrete element model simulation of concrete specimens under uniaxial compression,

[DOI: 10.22068/IJCE.13.3.245]

Engineering Fracture Mechanics 110, 2013, pp. 81-98.
[11] Tran VT, Donzй FV, Marin P. A discrete element model of concrete under high triaxial loading, Cement & Concrete Composites, 2011, Vol. 33, pp. 936-948.
[12] Kunhwi Kim, Yun Mook Lim, Simulation of rate dependent fracture in concrete using an irregular lattice model, Cement & Concrete Composites, 2011, Vol. 33, pp. 949-955.
[13] Gianluca Cusatis, Daniele Pelessone, Andrea Mencarelli. Lattice discrete particle model (LDPM) for failure behavior of concrete, Cement & Concrete Composites, 2011, Vol. 33, pp. 881-890.
[14] Hyunwook Kim, William G. Buttlar, Discrete fracture modeling of asphalt concrete, International Journal of Solids and Structures, 2009, Vol. 46, pp. 2593-2604.
[15] Schlangen E, Koenders EAB, Van Breugel K. Influence of internal dilation on the fracture behavior of multi-phase materials, Engineering Fracture Mechanics, 2007, Vol. 74, pp. 18-33.
[16] Mier V, Vliet V. Influence of microstructure of concrete on size/scale effects in tensile fracture, Engineering Fracture Mechanics, 2003, Vol. 70, pp. 2281-2306.
[17] Bloander JE, Saito S. Fracture analysis using spring networks with random geometry, Engineering Fracture Mechanics, 1998, No. 5, Vol. 61, pp. 569-591.
[18] Landis EN, Bolander JE. Explicit representation of physical processes in concrete fracture, Journal of Physics D: Applied Physics, 2009, No. 21, Vol. 42, pp. 17.
[19] Rossi P, Ulm FJ, Hachi F. Compressive behavior of concrete: physical mechanisms and modeling, Journal of Engineering Mechanics, 1996, No. 11, Vol. 122, pp. 1038-1043.
[20] Camborde F, Donzé FV, Mariotti C. Numerical study of rock and concrete behavior by discrete element modeling, Computers and Geotechnics, 2000, No. 4, Vol. 27, pp. 225-247.
[21] Nagai K, Sato T, Ueda T. Mesoscopic simulation of failure of mortar and concrete by 2d RBSM, Journal of Advanced Concrete Technology, 2004, No. 3, Vol. 2, pp. 359-374.
[22] Wang Zh, Lin F, Gu Xi. Numerical simulation of failure process of concrete under compression based on mesoscopic discrete element model, Tsinghua Science and Technology, 2008, No. S1, Vol. 13, pp. 19-25.
[23] O'Rourke J. Computational Geometry in C. 2nd Ed., Cambridge, London, Cambridge University Press, 1998.
[24] Aslami M. Two dimensional numerical simulation of concrete in compression, Thesis (Master of Eng), Tehran, Iran, Iran University of Science and Technology, 2011.
[25] Nagai K, Sato Y, Ueda T. Numerical simulation of fracture process of plain concrete by rigid body spring method. In: Proceedings of the First FIB Congress 2002 - Concrete Structures in the 21st Century. Osaka, Japan, 2002, 8, pp. 99-106.
[26] Jing L, Stephansson O. Fundamentals of discrete element methods for rock engineering: theory and applications Elsevier, 2007.
[27] Cundall P, Strack O, A discrete numerical model for granular Assemblies, Geotechnique, 1979, No. 1, Vol. 29, pp. 47-65.
[28] Watanabe K, Niwa J, Yokota H, Iwanami M. Experimental study on stress-strain curve of concrete considering localized failure in compression, Journal of Advanced Concrete Technology, 2004, No. 3, Vol. 2, pp. 395-407.

[DOI: 10.22068/IJCE.13.3.245]